# Gust Alleviation of Aeroelastic Aircraft Using CFD Simulation

*Aleš Prachař*
*VZLU – Czech Aerospace Research Centre*
*Research Scientist*
*Beranových 130, 199 05 Prague, Czech Republic*
*prachar@vzlu.cz*

*Pavel Hospodář*
*VZLU – Czech Aerospace Research Centre*
*Research Engineer*

*Petr Vrchota*
*VZLU – Czech Aerospace Research Centre*
*Research Engineer*

## ABSTRACT

A CFD study of a gust alleviation technique based on the use of aircraft's control surfaces on the main wing and on the horizontal tail plane is presented. The NASA Common Research model of an airliner is used as the reference configuration. The gust model is based on adding artificial gust velocities into the governing equations, so-called Disturbance Velocity Approach. The gust is identified as a change in the Angle of Attack upstream of the aircraft nose. A series of gusts is used to measure response of the aircraft and to establish the dynamic gust model. The elasticity of the aircraft model is taken into account employing modal analysis and the response of the aircraft structure is studied. The movable control surfaces are defined and characterized by CFD using the mesh deformation technique in the unsteady RANS simulations. Finally, the dynamic model based on both the gust data on one hand and on the control surfaces on the other is exploited to define the controller with the aim to alleviate the gust. The required time response of the movable control surfaces is studied to clarify limits of this alleviation technique.

**KEYWORDS**: *CFD, gust response, moving control surfaces, NASA Common Research Model*

## NOMENCLATURE

Latin

| | |
|---|---|
| $C_{REF}$ | mean aerodynamic chord [m] |
| $C_L$ | lift coefficient [-] |
| $C_{LS}$ | sectional lift coefficient [-] |
| $C_m$ | pitching moment coefficient [-] |
| H | gust gradient distance [m] |
| Re | Reynolds number [-] |
| s | time scale, $s=V\ t/C_{REF}$ [-] |
| $u_g$ | gust velocity vector [m/s] |
| V | flight forward velocity [m/s] |
| x,y,z | streamwise, spanwise and normal coordinate [m] |

Greek

| | |
|---|---|
| δ | deviation |

## 1 INTRODUCTION

The gust, as a sudden and unpredictable disturbance of the airflow relative to the flight path, is a source of potential problems. Besides compromising passenger comfort, the gusts also cause severe problems for aircraft stability and control, and introduce additional forces exerted on the airframe.

The requirement for the aircraft to handle gusts is part of the certification process and is covered in detail in relevant regulations [2]. Both vertical (positive and negative) and lateral gusts have to be considered. We are focusing on upward vertical gusts, because they introduce additional stresses to the already loaded structure of the aircraft.
The gust is defined as the disturbance in the flowfield in the vertical direction, perpendicular to the flight path. It is characterized by its length and amplitude. The gust profile is given by the '1-cosine' shape, i. e., by the function

$$u_{g,z} = \frac{u_{ds}}{2}\left[1 - \cos\left(\frac{\pi x}{H}\right)\right], \quad 0 < x < 2H, \tag{1}$$

where the design gust velocity $u_{ds}$ is defined in the regulations and the gust gradient distance $H$ represents the half length of the gust, in other words the distance between the start of the gust and its peak. Such a disturbance in the free stream velocity is transported towards the aircraft, equivalently the aircraft flies into it. The range of gradient distances from $H$=9 to $H$=107 meters is required [2]. For the present case the gust envelope is shown in Fig. 1 with the length scale relative to the mean aerodynamic chord of the considered aircraft.

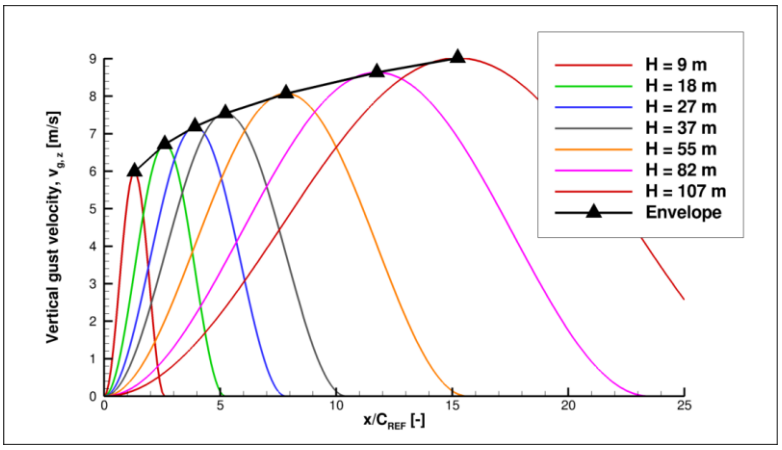


**Figure 1: Gust profiles and gust envelope.**

The methods for the gust detection range from accelerometer measurement on the airplane wings, which indicates irregularities in the flow by means of their action on the aircraft structure, to remotely sensing the gust, e. g., via Doppler LIDAR [5]. Various passive or active alleviation techniques are used to overcome or at least to reduce the effect of the gust. The gusts are also studied experimentally in the wind tunnel environment, as well as computationally, from simplified to advanced CFD methods [13]. Development of gust alleviation controllers often uses a dynamic model of an airplane. Since the development of the dynamic model is a challenging task [14], the study presented here employs CFD directly to evaluate aircraft responses at various conditions.
The idea behind this paper is to use aircraft's control surfaces to counteract the gust and to develop a controller for the control surfaces action based on the gust evaluation and identification. In the previous study [8] the case of rigid aircraft and uniform deflection of all control surfaces on the main wing was considered. In the present paper the method includes wing deformation obtained from the wing modal analysis coupled to the CFD solver. Furthermore, the control of the main wing control surfaces was split to improve the results.

## 2 DESCRIPTION OF MODEL PROBLEM AND ITS SOLUTION

To show the methodology the NASA Common Research Model (CRM) of the generic airliner [10] has been used, the same case was used for the Drag Prediction Workshops (3rd – 6th DPW) [1]. Although the CRM is defined as 'full scale model' ($C_{REF}$ = 7 m) in DPW, the wind tunnel model geometry and the structural model given in [7] is related to the wind tunnel model size ($C_{REF}$=0.189 m). The computational grid was found among the grids provided for the 4th DPW (DLR wing-body-tail coarse Solar grid with approximately 4.7 million grid points) and scaled to the model scale. The relatively

coarse computational grid was chosen to save computational resources due to the need to perform several time-resolved (unsteady) calculations.
The case of the cruise flight with the velocity M=0.85, operating at the design $C_L$=0.5 is considered. The Reynolds number based on $C_{REF}$ is Re=5 million as used for the wind tunnel measurements [7] and also for the DPW.
During previous studies it has been found that the wind tunnel model deformation, in particular the main wing deformation, plays an important role in the comparisons made between the CFD results and wind tunnel results [11]. This is true even when the WT model is usually much stiffer than the real aircraft. The structural model used in this study was developed for the WT model [7] and it is not intended to mimic elastic behavior of the real aircraft. Only the main wing was considered flexible, the structural model was analyzed with the aid of MSC NASTRAN software, the first 20 mode shapes were obtained from the modal analysis. The aeroelastic deformation is obtained from the solution of the system of equations,

$$M_n\ddot{q}_n + C_n\dot{q}_n + K_n q_n = Q_n, \quad n = 1..N, \tag{2}$$

where $M_n$, $C_n$ and $K_n$ are the generalized mass, damping and stiffness coefficients for the n-th natural mode, and $Q_n$ is the generalized aerodynamic force.
The set of control surfaces were defined on the main wing and on the horizontal tail plane (HTP). The definition was done solely on authors' judgment, see Fig. 2. No special care was taken of proper dimensioning of the control surfaces. Besides elevator, aileron and flaperon, defined as the trailing edge devices as expected, the spoilers were also represented by trailing edge devices due to simplification of the CFD, since the spoiler deployment is too complicated in the CFD simulation.
The movement of the control surfaces is represented by the grid deformation of the wing trailing edge, which is smoothly connected to the rest of the wing. Thus, the gaps between the wing and the flap (cove, side cuts) are neglected. With this approach the movement of control surfaces is manageable with the mesh deformation technique implemented in the CFD code. The control surfaces are used to alleviate the gust response.

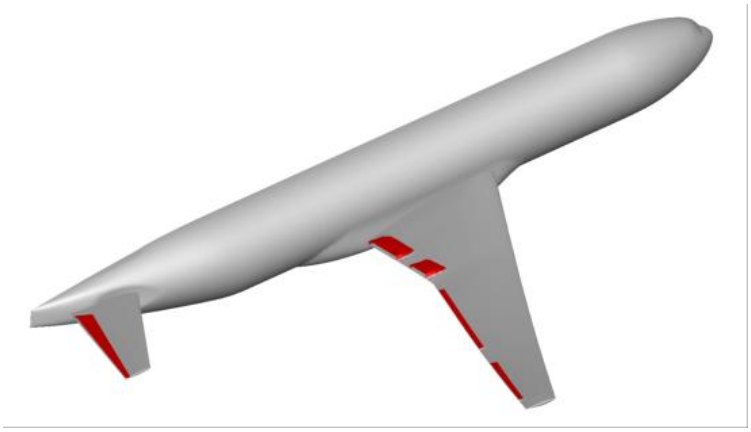

**Figure 2: NASA Common Research Model with defined control surfaces indicated by red colour.**

The gust model implemented in the CFD solver is based on the Disturbance Velocity Approach, validated among others in [6]. This model relies on the definition of artificial gust velocity introduced to the flow equations. For example, the continuity equation includes the contribution from the gust velocity,

$$\frac{d}{dt}\int_V \rho\, dV - \oint_S \rho(v - v_b - v_g)\cdot n\, dS = 0, \tag{3}$$

where $v_b$ is the velocity of boundary of the control volume. The advantage of this approach is that it can be used on standard CFD grids with no special requirements on the resolution in the far field.
Since the wind tunnel model size aircraft was used for the simulations, the gust lengths were also scaled accordingly to keep the ratio between the gust length and aircraft size ($C_{REF}$) the same as for

the full scale aircraft. Other gust parameters, as defined in [2], were roughly chosen according to the approximate properties of similarly sized aircraft. The case of vertical upward gust was selected.
The Edge [3] is the CFD code used for the presented simulations. All the simulations are carried out as unsteady RANS with Explicit Algebraic Reynolds Stress turbulence model [12]. The obtained unsteady data from the gust response and the control surfaces action are processed in MATLAB System Identification Toolbox. The dynamic systems are identified and feed-forward law is designed to prescribe control surfaces movement to counteract the gust effect.

## 3 COMPUTATIONAL RESULTS

### 3.1 GUST RESPONSE

To understand the gust dynamics and to identify the dynamic model, a series of CFD calculations was carried out for the selected gusts within the required range, cf. Fig. 3. The response of the aircraft was evaluated and decomposed to individual parts; the main wing, HTP and the fuselage. Besides integral values, like $C_L$ and $C_m$ evaluated on the aircraft parts, a more detailed analysis in terms of span-wise distribution of the lift and pitching moment deviation from the undisturbed flight was also performed and used in the study. The $\delta C_L$ and $\delta C_m$ are compared to the case of rigid aircraft response [8] in Fig. 3. As we can see, while gust amplitude varies by at most 30% (Fig. 1), the $C_L$ increments by a factor of 4 in the prescribed gust length range. There is an interesting $C_m$ dependence with maximum deviation at medium-length gusts which is due to the gust interaction with the fuselage. The line colors in Fig. 3 represent results for the gusts of different lengths, cf. Fig. 1.

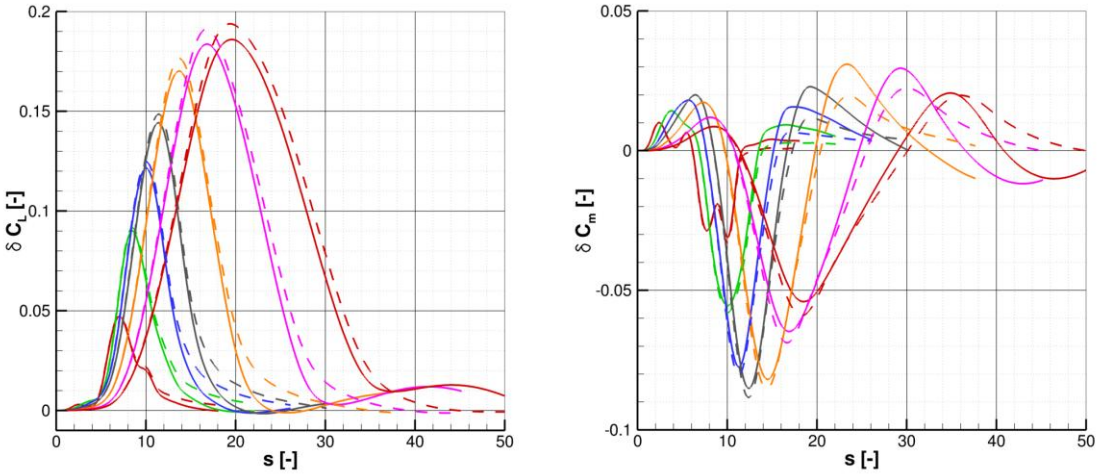


**Figure 3: Response of the rigid (dashed) and elastic (solid line) aircraft to the gust, $C_L$ (left) and $C_m$ (right).**

The difference between rigid and flexible aircraft response to the gust can be seen in slight reduction of the gust response peak and in the aeroelastic response generated by the gust. Structural response related in general to the first two natural modes is in this case slower than the gust itself. Hence, the gust acts as an excitation which disturbs the structure which is then slowly damped. The effects of aeroelasticity measured by the integral characteristics are in general an order of magnitude below the gust influence.
The transport delay between gust acting on the main wing and on the HTP is clearly visible, cf. Fig. 4. While HTP contribution to the total $C_L$ is minor, the $C_m$ augmentation is more significant due to long moment arm. There is also time lag between gust acting on the inboard part of the wing and the wing tip due to the wing sweep.

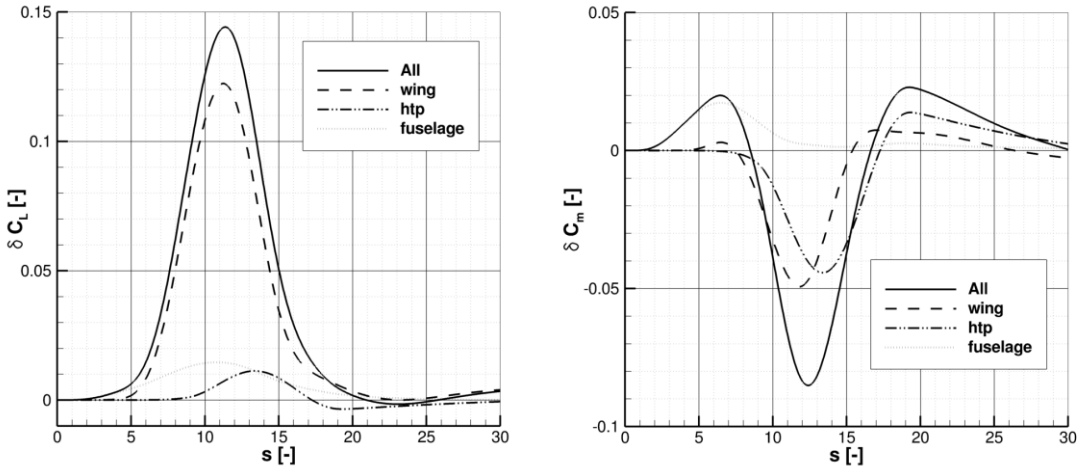


**Figure 4: Detailed decomposition of the $C_L$ and $C_m$ coefficients evolution.**

## 3.2 CONTROL SURFACES CHARACTERIZATION

The '1-cosine' input signal to the control surfaces was prescribed for the movement of control surfaces described earlier (Fig. 2) and the response was evaluated for two frequencies in the range of expected input for the gust alleviation. Each control surface was considered independently and the main wing span-wise force distribution of the response was evaluated.

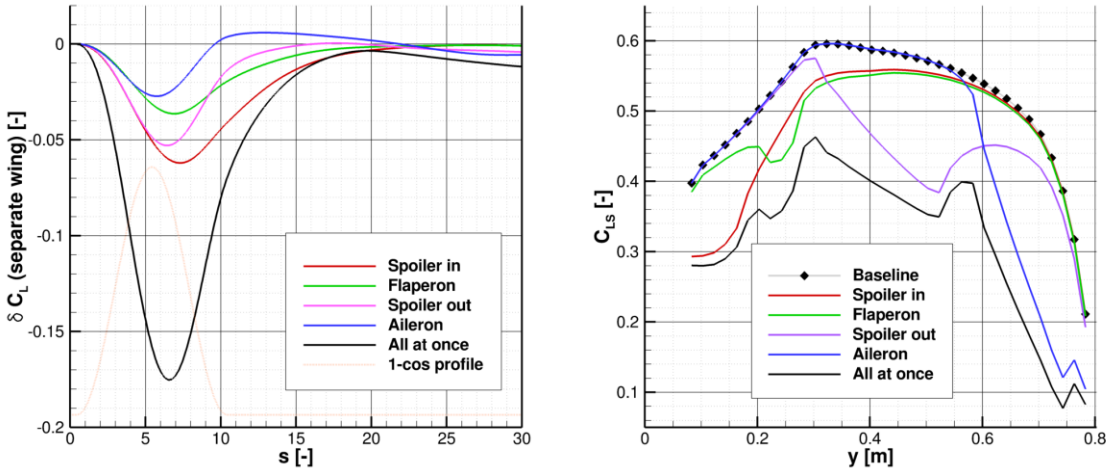


**Figure 5: Time evolution of the wing $\delta C_L$ (left) and spanwise distribution of $C_{LS}$ at peak deflection time instant, *s=5.5*.**

We observe that the control surface deflection changes local sectional lift coefficient (evaluated from local cuts) mostly in the region between its location and the wing tip. Moreover, a time lag between maximum deflection and the largest $\delta C_L$ peak is observed, the largest one for inboard control surfaces, since there is a certain time needed for the disturbance caused by the control surface to propagate towards the wing tip. We also observe that while for inner control surfaces the $C_L$ returns to the starting value after a short time, the outboard control surfaces induce aeroelastic response which causes slow oscillation of the $C_L$.

### 3.3 DYNAMIC SYSTEM IDENTIFICATION

The obtained data served as a basis to set up control laws to prescribe control surfaces movement based on measured gust, identified as the change in the angle of attack. Both systems, gust response and controls deflection, were identified using System Identification Toolbox in Matlab. Time delay in gust dynamics plays significant role in feed-forward control. It provides a time slot to compute controls deflection. Dynamics of control each deflection (aileron, flaperon, spoilers) was identified independently.

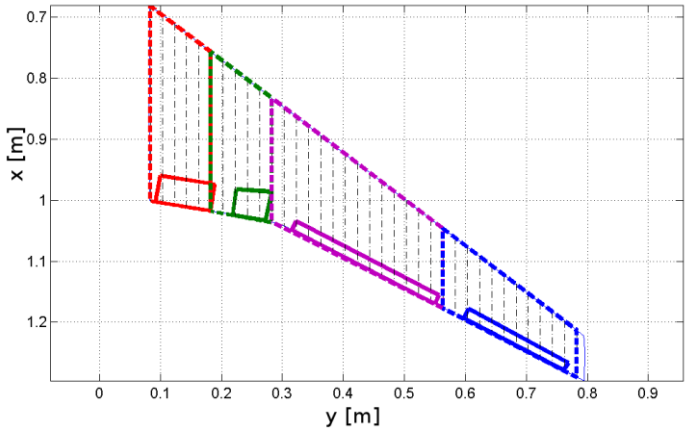


**Figure 6: Main wing divided into sections.**

The gust response identification was performed separately on the wing sections enclosing each of the control surfaces, see Fig. 6 and 7. The dynamic model formula used for each of the sections remained the same, only different coefficients were sought. The reason that inboard sections are better matched can be explained by the elasticity of the wing, which is more pronounced at the outboard sections.

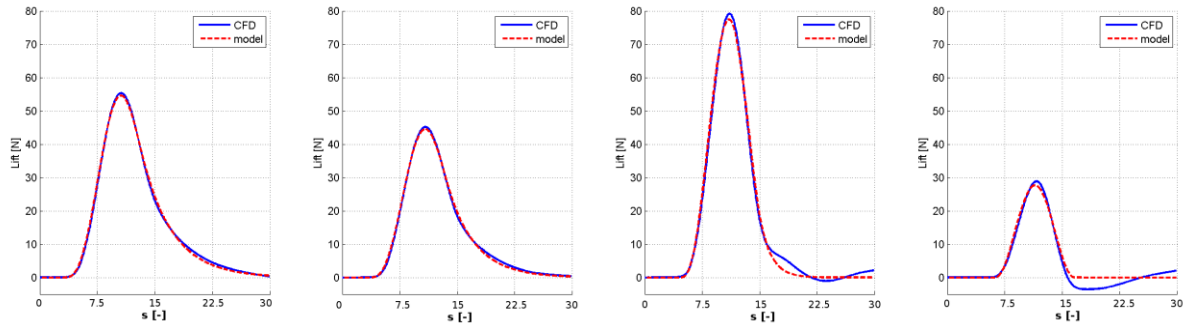


**Figure 7: Gust response identification for individual main wing sections (inboard - left, outboard - right).**

Similar identification was performed for the active control surfaces. The response of each of the control surfaces was measured and the dynamic model was identified with respect to wing sections. The dynamic model becomes rather complicated because of the fact that the whole outboard part of the wing is influenced by the control surface action.

Only the feed forward control procedure was used in this case [9]. Hence, there is no correction during the control. The whole control signal is defined without responding to how the system actually reacts. The strategy of this control system is based on the identified disturbance (S) and control (C) dynamic. Control input is then computed as follows:

$$\alpha \cdot S = C_L, \quad \delta \cdot C = C_L, \quad \alpha \cdot S + \delta \cdot C = 0, \quad \delta = -\alpha \cdot \frac{S}{C}. \tag{3}$$

The simplified scheme of the controller is presented in Fig. 8. However, the system (C1) is rather complicated and incorporates independent sub-systems related to individual control surface dynamics and its effect (again separated to individual wing sections) on the lift distribution. Based on the previous experience, the main wing control surfaces are responsible for alleviation of the gust induced increase of the lift measured again only on the main wing. The elevator is used in order to control the overall pitching moment.

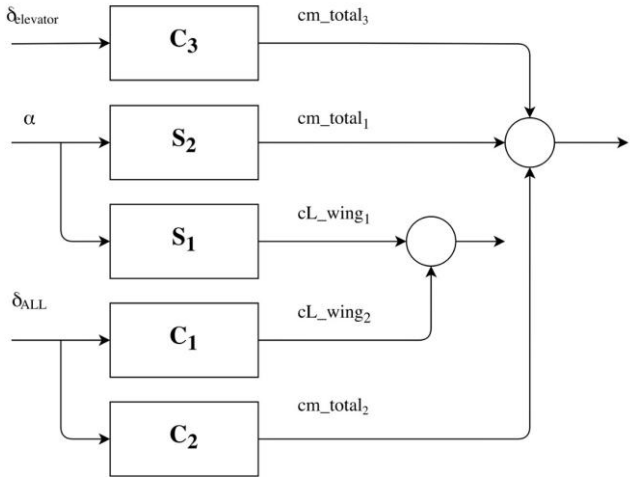


**Figure 8: Simplified scheme of the controller.**

### 3.4 GUST ALLEVIATION SIMULATION

The proper identification of the dynamic systems enables the controller to prescribe movement of the control surfaces in order to reduce influence of the gust. The case simulated again with the CFD, employing all ingredients together: CFD simulation of elastic wing case with gust model and control surfaces movement based on the presented controller. This was done in several steps.
First, the main wing control surfaces were controlled with one input signal, i.e., the control surfaces move together with the same deflections. The second case includes independent main wing control surfaces. It can be seen that significant improvement of the main wing $\delta C_L$ results were achieved, see Fig. 9. The span-wise distribution of $C_{LS}$ shows that more appropriate distribution was achieved with independent control surfaces (blue line). When all control surfaces move together (green line, Joint), negative $\delta C_{LS}$ is present at the wing tip in the early phase since the aileron starts to move upward before even the gust reaches the outboard part of the swept wing (Fig. 9, left).

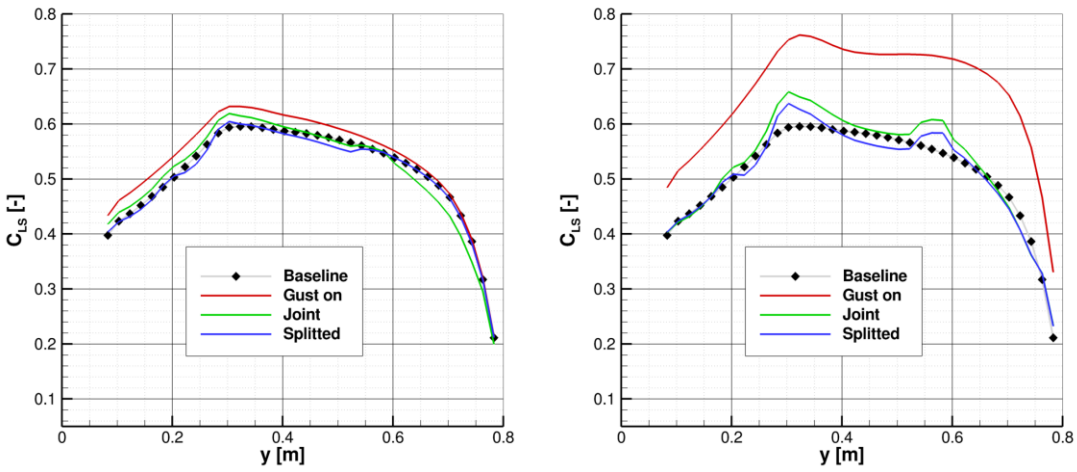


**Figure 9: Spanwise $C_{LS}$ distribution for two time instances. Initial phase of the gust action (left), maximum loading for the uncontrolled case (right).**

The integral values are visible in Fig. 10. We observe that the overall lift and pitching moment increase was reduced by about 90%, similar to what was observed in the rigid case [8]. Only the case with independent controls was shown here for the sake of clarity.

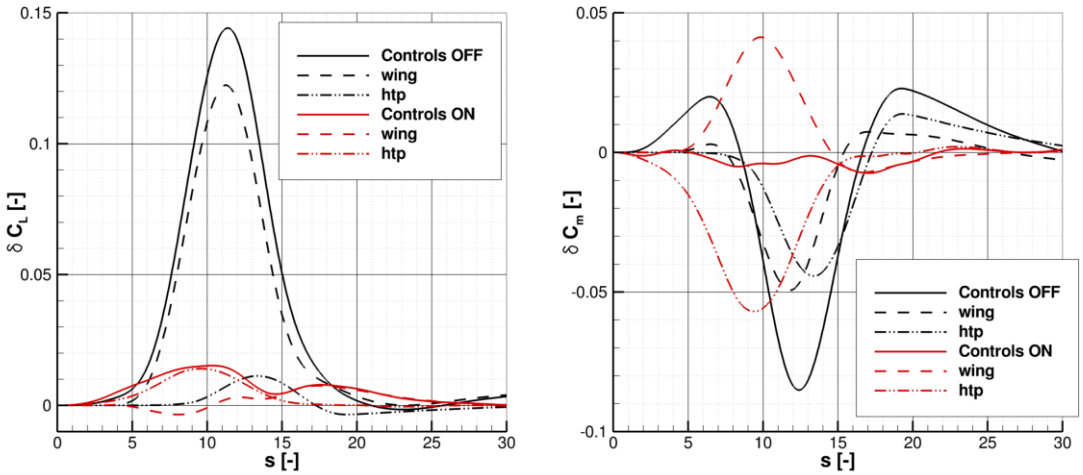


**Figure 10: Comparison of the uncontrolled case (black) with splitted controls (red).**

Since the aeroelastic simulation was performed, it was possible to evaluate wing bending and wing twist in the post-processing phase. In accord with the results presented in [11] we observe in Fig. 11 that in comparison with the unloaded geometry during the undisturbed flight the main wing was bent by about 16.4 mm (vertical deflection of the quarter chord point of the main wing end cut) and twisted by about 1.2 degrees. The effect of the gust causes additional bending of nearly 5 mm and 0.5 degrees in twist. Reduction of the main wing lift increase has, moreover, positive effect on the reduction of wing vibrations in terms of their amplitude. As already mentioned, the elastic effects have much larger time scales compared to the gust passage, therefore the simulation were truncated before the vibrations disappeared.

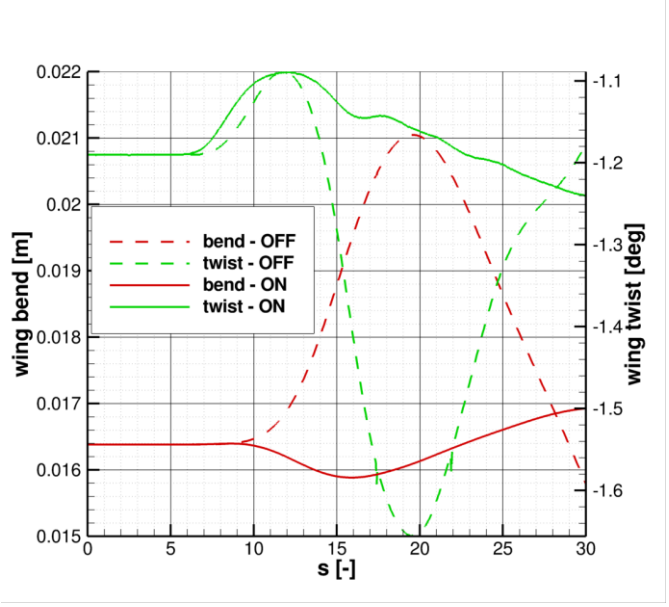


**Figure 11: The main wing twist (green) and bend (red), measured at the wing tip, for uncontrolled case (dashed) and with independent controls (solid).**

## 4 CONCLUSION

Computational study of the gust alleviation using active control surfaces was presented. Although only forward control system was used, the maximum increment of the lift and pitching moment was reduced by an order of magnitude. Such a promising result can be attributed to exact knowledge of the gust position, it's a priori known shape and the system identification focused on the chosen gust length case.
The aeroelastic effect was studied using modal decomposition. The reduction of the wing bending and wing twist was observed, although it was not considered to be a parameter that has to be taken care of.
The next steps could be incorporation of the feedback loop based, e. g., on the probe showing deformation of the wing or on local pressure variation values. The simulation of the aircraft maneuver caused by the gust within the same CFD environment would also move the methodology significantly higher.
After all, the multi-disciplinary add-ons to the standard CFD analysis are one of the reasons of this study. The communication between the CFD code and other systems, such as gust modeling, aeroelasticity, control surfaces controller, in the future possibly also maneuvering, done "on-line" during the course of the simulation is an important extension and the added value to the classical CFD analysis.

## ACNOWLEDGMENTS

This research was supported by The Ministry Industry and Trade of the Czech Republic for long term strategic development. Access to computing and storage facilities owned by parties and projects contributing to the National Grid Infrastructure MetaCentrum, provided under the programme "Projects of Large Infrastructure for Research, Development, and Innovations" (LM2010005), is greatly appreciated.

## REFERENCES

1. AIAA Drag Prediction Workshop, web page; 2017 retrieved 18th July 2017; https://aiaa-dpw.larc.nasa.org
2. EASA; 2007; "Certification Specifications for Large Aeroplanes (CS-25). Amendment 3"; European Aviation Safety Agency; September 2007.
3. Eliasson, P.; 2002; "Edge, a Navier-Stokes solver for unstructured grids", in Proceedings to Finite Volumes for Complex Applications III., pp. 527–534. ISTE Ltd., London.
4. Eliasson, P., Peng, S.-H. and Tysell, L.; 2013; "Computations from the fourth drag prediction workshop using the Edge solver"; *Journal of Aircraft*, **50**, 5; pp. 1646–1655.
5. Fezans, N., Schwithal, J. and Fischenberg, D.; 2017; "In-flight remote sensing and identification of gusts, turbulence, and wake vortices using a Doppler LIDAR"; *CEAS Aeronaut J* **8**, 313. doi:10.1007/s13272-017-0240-9
6. Heinrich, R. and Reimer, L.; 2014; "Simulation of Interaction of Aircraft and Gust Using the TAU-Code", in: *New Results in Numerical and Experimental Fluid Mechanics IX*, Springer.
7. NASA Common Research Model web page, retreived 18th July 2017, https://commonresearchmodel.larc.nasa.gov/
8. Prachař, A., Hospodář, P., Vrchota, P.; 2017; "Gust alleviation of NASA Common Research Model Using CFD", In *Proceedings to Engineering Mechanics 2017*, Svratka, Czech Republic
9. Stevens, B., I., Lewis, F., L.; 1992; "Aircraft Control and Simulation". John Wiley and Sons, ISBN 0471613975
10. Vassberg, J. C., DeHaan, M. A., Rivers, M. B., and Wahls, M. S.; 2008; "Development of a Common Research Model for Applied CFD Validation Studies", *AIAA Paper 2008-6919*.
11. Vrchota, P., Prachar, A., Šmíd, M.; 2017; "Improvement of Computational Results of NASA Common Research Model by Modal Analysis", *Journal of Aircraft*, **54**, 4, pp. 1294-1302. DOI: 10.2514/1.C033952

12. Wallin, S. and Johansson, A. V.; 2000; "An Explicit Algebraic Reynolds Stress Model of Incompressible and Compressible Flows", *Journal of Fluid Mechanics*, **43**, 9, pp. 89-132.
13. Zaide, A. and Raveh, D. E.; 2006; "Numerical Simulation and Reduced-Order Modeling of Airfoil Gust Response", *AIAA Journal*, **44**, 8, pp. 1826-1834.
14. Ghoreyshi M., Post M., Cummings R., Da Ronch A., and Badcock K; 2012; "Transonic Aerodynamic Loads Modeling of X-31 Aircraft", 30th AIAA Applied Aerodynamics Conference, Fluid Dynamics and Co-located Conferences